A Theory of Domain Creation and Coercive Force in Polycrystalline Ferromagnetics*†

JOHN B. GOODENOUGH‡
Lincoln Laboratory, Massachusetts Institute of Technology, Cambridge, Massachusetts
(Received December 17, 1953; revised manuscript received April 30, 1954)

Granular inclusions, grain boundaries, lamellar precipitates, and the crystalline surface have been examined as possible nucleation centers for domains of reverse magnetization in ferromagnetic materials. It is concluded that the surface density of magnetic poles at the grain boundaries ω^* is the most common source of nucleation energy in polycrystalline materials.

The concept of nucleation of domains of reverse magnetization has led to a calculation of three more terms which may contribute to the coercive force in polycrystalline materials, *viz.*, a grain-boundary, a lamellar-precipitate, and a domain-wall-surface-tension contribution.

The theoretical predictions are compared with several old experiments. New insight is gained on the problem of stress sensitivity of polycrystalline ferromagnetics and *B-H* loop shape.

I. INTRODUCTION

CURRENT magnetic-domain theory and experiment has shown that if a magnetic specimen, which is not finely divided, is in a strong, external, slowly alternating magnetic field, then the induced change in magnetic flux through the sample is primarily due to the motion of domain walls. In order to understand the characteristics of any *B-H* hysteresis loop, it is necessary to know the origins of the individual domain walls and the factors which hinder their motion through the sample when driven by an external magnetic field.

The principal cause of flux change may be assumed to be the motion of 180° domain walls if the specimen does not have a special geometry or orientation of its axes of easy magnetization which would energetically favor the creation of many domains at right angles to the applied field. It will be assumed that the specimen has a cubic lattice, is polycrystalline, and is in the form of a toroid or of a long rod parallel to the applied field.

If a specimen is saturated, no domain walls exist within it. If the flux in a saturated sample is to be reversed by the motion of 180° domain walls, domains of reverse magnetization must first be created. The new domains will be bounded by 180° walls, and as any domain grows in the presence of a favorably oriented external field, its boundary walls will move.

If an external field, which has saturated a magnetic specimen, is reduced and reversed, domains of reverse magnetization may be created in several regions of the specimen before irreversible wall motion, or irreversible domain growth, begins. H_{ni} will be defined as the critical field strength for domain creation in any ith region of the specimen. It will be defined as positive if it is oriented in the direction of the magnetization within the new domain.

If all $H_{ni}>0$, the difference in induction between saturation, B_s, and the remanence, B_r, is given by the rotation of the elementary atomic moments from the external-field direction to a crystallographically preferred direction of magnetization. If some $H_{ni}<0$, however, there is a further reduction of the remanence which is proportional to the volume of material which is included in the reverse domains. In order to obtain a material of high retentivity, therefore, one requirement is that all $H_{ni}>0$.

If the induction is reversed by the irreversible motion of 180° domain walls, the coercive force will usually represent some average critical field for irreversible wall motion. H_{wi} will be defined as the critical field strength for irreversible motion of the domain walls which enclose the ith domain of reverse magnetization. If all $H_{ni}>H_{wi}$, the *B-H* loop will be square because a domain of reverse magnetization, once created, will be in an external field of sufficient magnitude to drive its boundaries across the specimen. If the $H_{wi}\gg H_{ni}$ and if the H_{ni} are randomly spread over a wide range of H about some mean value, the *B-H* loop will have rounded shoulders, shallow-sloping sides, and a large coercivity.

The domain-wall contribution to the initial permeability of a sample is proportional to the area of 180° walls which are present within the specimen at zero net magnetization. If many domains exist, the total domain-wall area will be large. It is also inversely proportional to the force which holds these walls to a given location within the sample. H_{wi} gives a measure of this force. A high-initial-permeability material will contain a large area of domain wall which has low H_{wi}.

A knowledge of H_{ni} and H_{wi} is therefore of great practical importance as well as of theoretical interest. In Secs. II and III some of the factors which contribute to H_{ni} and H_{wi} are considered theoretically. In Sec. IV the theoretical predictions are compared with experiment.

II. MAGNETIC-DOMAIN CREATION

Domains of reverse magnetization are created at lattice imperfections. An examination of those imper-

* The research reported in this document was supported jointly by the Department of the Army, the Department of the Navy, and the Department of the Air Force.

† This paper contains the work that was reported in Phys. Rev. 91, 434 (1953).

‡ Staff Member, Lincoln Laboratory, Massachusetts Institute of Technology, Cambridge, Massachusetts.

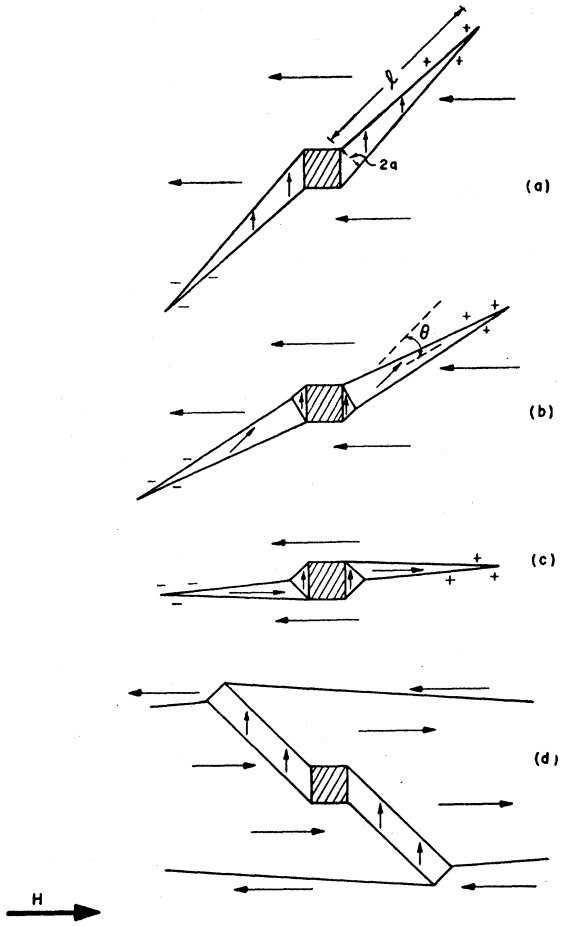

FIG. 1. The creation and growth of a domain of reverse magnetization by the rotation of a closure domain at an inclusion.

fections which might act as the nucleating centers for new domains suggests the study of granular inclusions, lamellar precipitates, grain boundaries, and the crystalline surface. The field strength at which the new domains are formed, H_n, and, where pertinent, the field strength at which the new walls are moved irreversibly away from the imperfection, H_w, will be considered for each of these cases.

A. The Granular Inclusion

(1) In many lattices there is a large density of inclusions present. These inclusions may be precipitates of another phase, impurity aggregates, or voids. Néel[1] predicted that in lattices with three axes of easy magnetization closure domains form about inclusions, as in Fig. 1(a), in order to reduce the energy associated with the magnetic poles at the inclusion surfaces. Williams[2] has observed these closure domains in colloidal-magnetite patterns on polished surfaces of metals.

Only those inclusions whose radius is larger than a critical size R_c will have closure domains about them. In Appendix I it is shown that $R_c \approx 10^{-5}$ cm in iron. In the ferrites which have a low saturation magnetization I_s, however, it is possible that $R_c \approx 10^{-3}$ cm. If an inclusion is too small to support a closure domain, it will not act as a nucleating center for a domain of reverse magnetization.

In order that an inclusion with closure domains act as a nucleating center for a domain of reverse magnetization, the closure domains must be rotated through 45° by the external field. The domain of reverse magnetization can then grow as shown in Fig. 1. In Appendix II it is shown that, for inclusions in materials with three axes of easy magnetization, $H_n > 10$ oersteds. Since this is larger than the coercivity of most soft magnetic materials, it is concluded that these inclusions are not imperfections at which 180° domain walls are created. It will be shown in Sec. III, however, that the presence of the inclusions does influence the coercive force.

(2) Williams and Goertz[3] have observed domains of reverse magnetization at large inclusions in a perminvar ring with only one axis of easy magnetization. These domains formed as shown in Fig. 2(a). In order to estimate the nucleation field strength, it is assumed that the energy of the surface poles after domain formation is much less than before. Then, since there is no magnetostrictive energy associated with the domains of reverse magnetization,

$$\frac{8\pi^2}{9}I_s^2R^3=\frac{\pi^2R^2}{2\lambda}\sigma_w+\frac{16\pi^2\eta}{3\sqrt{2}}\lambda[\ln(2/\lambda)-1]I_s^2R^3 - 2H_nI_s\cos\theta\frac{2\pi R^3}{3\sqrt{2}\lambda},$$

where R is the radius of the inclusion, θ is the angle between the applied field H and the magnetization, and $\lambda=R/\sqrt{2}l\ll 1$ is the ratio of the semiminor to semimajor axes of the domain of reverse magnetization which, for simplicity, is assumed a prolate ellipsoid. The critical field strength for domain creation is then

$$H_n=\left\{\frac{9}{16}\left(\frac{\sigma_w}{RI_s^2}\right)+3\sqrt{2}\lambda^2\eta[\ln(2/\lambda)-1]-\lambda\right\}\frac{2\sqrt{2}\pi}{3\cos\theta}I_s$$

$$\approx\left[1.7\left(\frac{\sigma_w}{RI_s^2}\right)-0.18\right]I_s \quad \text{for } \lambda\approx 1/30,\ \eta=0.1. \quad (1)$$

In iron if $R>10^{-5}$ cm, Eq. (1) gives $H_n<-10$ oersteds. It is concluded that if the radius of an inclusion in a material with one axis of easy magnetization is large ($R>10^{-5}$ cm in metals or 10^{-3} cm in ferrites), $H_n\ll 0$. If the inclusion density is low, the fractional volume of

[1] L. Néel, Cahiers phys. **25**, 21 (1944).
[2] H. J. Williams, Phys. Rev. **71**, 646 (1947).
[3] H. J. Williams and M. Goertz, J. Appl. Phys. **23**, 316 (1952).

material which is enclosed by such domains of reverse magnetization is small.

A more significant field strength to be examined, perhaps, is the critical field H_w at which the reverse-domain walls move irreversibly away from the inclusion which generated them. The principal resistance to the growth of an inclusion-nucleated reverse domain comes from the energy associated with the inclusion-surface magnetic poles. If the inclusion is so small that the reverse domain grows away from the inclusion without the formation of a new domain within the reverse domain, then

$$2H_wI_s\cos\theta\Delta V=(8\pi^2/9)I_s^2R^3+\sigma_w\Delta A_w+\Delta E_d;$$

$$H_w\approx[0.9(\sigma_w/RI_s^2)+0.05]I_s \text{ for } \lambda\approx 1/30,\ \eta=0.1. \quad (2)$$

Even in the ferrites this is a high field strength. At inclusions of larger radius, the domain will be free to grow irreversibly if a second domain of reverse magnetization is created inside the first (see Fig. 2). The inner domain can then grow to balance the poles on the surface of the inclusion as the original domain walls move away. H_w is therefore calculated in Appendix III as the field strength at which a second domain of reverse magnetization is created inside the first. It is found that

$$H_w>I_s\{0.005+0.13R_c/R\}, \quad (3)$$

where R_c is the critical radius of an inclusion for reverse-domain formation in zero external field. Unless $R_c/R\ll 1$, Eq. (3) gives, for soft magnets, $H_w>H_c$. These domains do not, in general, contribute 180° walls which move irreversibly through a magnetic material to reverse its flux.

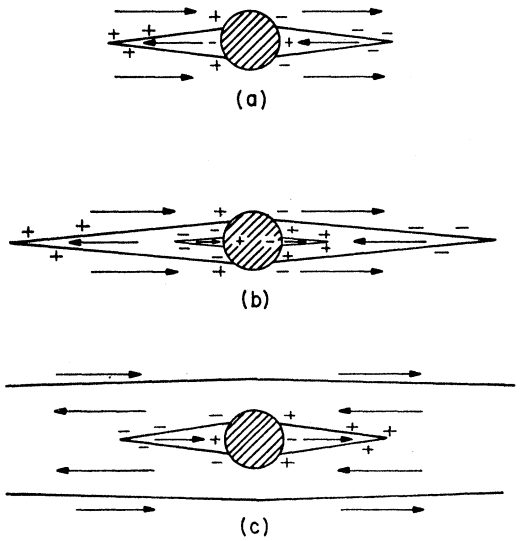

FIG. 2. Schematic representation of the growth of a domain of reverse magnetization away from an inclusion in a parallel, external field H. The crystal has but one axis of easy magnetization.

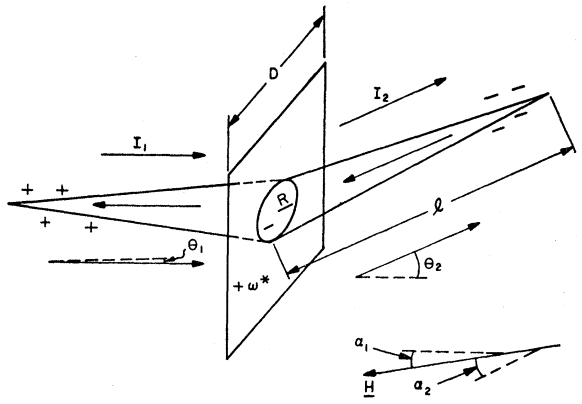

FIG. 3. Schematic nucleation of a domain of reverse magnetization at a grain boundary.

B. Lamellar Precipitates and Grain Boundaries

For ease of calculation the grain boundary will be considered planar. It is therefore considered together with the lamellar-precipitate imperfection. A crystal lattice is, in general, anisotropic with regard to ease of magnetization. If a crystal is not under tensile stress, this anisotropy is determined by the crystallographic configuration. The grain boundaries in a polycrystalline specimen separate regions of different crystallographic orientation or easy-magnetization direction. At low field strengths, the magnetization vectors of the neighboring grains are not rotated from their easy-magnetization directions into complete alignment. Consequently there is generally a discontinuity across the boundaries in the magnetization-vector component normal to the boundary. Therefore magnetic poles exist at the grain boundaries, and magnetic energy is associated with these poles. If θ_1 and θ_2 are the angles made by the spontaneous-magnetization vector I_s of the neighboring grains and the normal to their common boundary, the grain-boundary-surface pole density is $\omega^*=I_s(\cos\theta_1-\cos\theta_2)$.

Similarly there will be magnetic energy associated with the poles which exist at the planar surface of a lamellar precipitate. If I_p is the spontaneous magnetization of the precipitate and α_s, α_p are the angles the normal to the lamellar plane makes with I_s and I_p, the lamellar-surface pole density is $\omega_l^*=(I_s\cos\alpha_s-I_p\cos\alpha_p)$. The angle α_p will so adjust itself as to minimize the energy associated with ω_l^* and the anisotropy of the precipitate.

The magnetic energy associated with these surfaces of magnetic poles would be reduced if domains of reverse magnetization existed to produce a pole distribution of alternating sign. This is illustrated in Fig. 3. Work must be done, however, in the formation of the domains of reverse magnetization. The grain boundaries or lamellar precipitates will act as nucleating centers for domains of reverse magnetization only if the

resulting reduction in energy is larger than the work required to form the domains.

In order to determine the critical field strength for domain creation at a planar surface of surface magnetic-pole density ω^*, further simplifying assumptions are made. First the applied field H is assumed to be so small and the anisotropy constant K so large that the magnetization in any domain is directed along an easy axis of magnetization. A subsequent correction (see Appendix IV) for this assumption does not, in zero approximation, alter the calculated critical field strength. Secondly the surfaces containing magnetic poles are assumed so far apart that the magnetostatic interactions between them can be neglected. It is further assumed that when reverse-domain creation occurs, it occurs periodically over the planar surface with elementary area D^2. The domains of reverse magnetization are taken to be prolate ellipsoids of semimajor axis l and semiminor axis $r<D$ such that $\lambda=r/l\ll 1$. The angles θ_1 and θ_2 are assumed small so that the two halves of the domain of reverse magnetization can be considered to have a common major axis in the estimation of the demagnetization factor $N=4\pi\lambda^2[\ln(2/\lambda)-1]$, the volume $V=4\pi r^2 l/3$, and the surface area $A_w=\pi^2 rl$. The change in internal energy of the crystal due to reverse-domain creation is then given by

$$\Delta E=(\sigma_0-\sigma_n)A_s-n[\sigma_w A_w+2NI_s^2V - HI_s(\cos\alpha_1+\cos\alpha_2)V+E_p+E_{np}], \quad (4)$$

where n is the number of domains of reverse magnetization created on the area A_s of planar surface. The surface-energy densities σ_0, σ_n, σ_w refer, respectively, to the grain boundary before and after nucleation has taken place and to the 180° Bloch walls. The demagnetization energy is $2NI_s^2V$, and α_1, α_2 are the angles the external field H makes with the direction of easy magnetization in the two neighboring grains. The interaction energies of the Bloch-wall poles with the plane-surface poles and with the neighboring Bloch-wall poles are, respectively, E_p and E_{np}.

The nucleation field strength H_n is that for which the change in free energy, $\Delta F=\Delta E-T\Delta S$, between the prenucleated and post-nucleated state vanishes. If $D=br$ and $b\lambda\ll 1$, then (see Appendix IV)

$$\Delta F=\frac{A_s I_s^2 l}{b^2}\left\{(\gamma_0-\gamma_n)\lambda-\frac{a\gamma_w}{r}-\gamma_p\lambda^2+\gamma_H+\gamma_S\frac{V_t}{r^2 l}\right\}, \quad (5)$$

where a is the distance between atoms whose magnetic moments give rise to the magnetization of the specimen and V_t is the total volume of the material. The dimensionless parameters γ_n, γ_w, γ_H, and γ_S are independent of r whereas $\gamma_0\propto 1/r$. The dimensionless parameter γ_p is, for $\lambda\ll 1$, dependent upon r only through the $\ln(2/\lambda)$. The parameter γ_p varies slowly with r and is, therefore, assumed independent of r. Since $n=A_s/D^2=A_s/(br)^2$, the optimum value of n is obtained by setting $\partial(\Delta F)/\partial r=0$ for a given value of l. This gives a relationship between the parameters, *viz.*,

$$-\gamma_p\lambda^2=\tfrac{1}{2}\gamma_n\lambda-\tfrac{1}{2}a\gamma_w/r+\gamma_S V_t/(r^2 l),$$

which, when substituted into Eq. (5) under the condition $\Delta F=0$, yields the nucleation field strength

$$H_n\cong\frac{3b^2\{(3\pi^2\sigma_w/2b^2\lambda)-(\sigma_0-\sigma_n/2)-(2T\Delta S/A_s)\}}{4\pi I_s l(\cos\alpha_1+\cos\alpha_2)}. \quad (6)$$

If typical values of l_m, V, and λ are chosen, where l_m is an average distance between planar surfaces of magnetic poles, at room temperatures

$$\frac{2T|\Delta S|}{A_s}\Big/\frac{3\pi^2\sigma_w}{2b^2\lambda}\ll 1.$$

Although the entropy term will be of increasing importance as the Curie temperature is approached, at room temperatures it can be neglected compared to the other terms. Also $\sigma_n\ll\sigma_0$ and is neglected. The nucleation field strength reduces, therefore, to

$$H_n\approx\frac{3b^2\{(3\pi\sigma_w/2b^2\lambda)-\sigma_0/\pi\}}{4I_s l(\cos\alpha_1+\cos\alpha_2)}. \quad (6')$$

It has been pointed out that a condition for a high retentivity is $H_{ni}>0$. If $\lambda=1/30$, the requirement that $H_n>0$ gives the condition

$$\sigma_0/\pi<(3\pi/2b^2\lambda)\sigma_w\approx 20\sigma_w\approx 80[A(K+\lambda_i\sigma)]^{\frac{1}{2}}, \quad (7)$$

where K is the anisotropy constant and $A=2JS^2/a$ is the usual exchange parameter.[4] It can be shown[5] that, for a cylindrical wall in a b.c.c. lattice, $\sigma_w\approx 4[A(K+\lambda_i\sigma)]^{\frac{1}{2}}$, where λ_i is the isotropic magnetostrictive constant and σ is the internal stress at the wall. Numerical factors of order unity are neglected.

If the planar surface is a grain boundary with surface pole density $\omega^*=I_s(\cos\theta_1-\cos\theta_2)$, the surface energy density (see Appendix V) is $\sigma_0\approx(1/3)\pi\omega^{*2}L$, where L is a mean grain diameter. Equation (7) then becomes

$$LI_s^2(\cos\theta_1-\cos\theta_2)^2<60\sigma_w\approx 240[A(K+\lambda_i\sigma)]^{\frac{1}{2}}. \quad (7')$$

This relationship is satisfied in metals if $(\cos\theta_1-\cos\theta_2)$ is made extremely small. A square B-H loop is commonly obtained in metals by reducing this factor by means of grain orientation, magnetic anneal, or application of tensile or compressive stress to materials with large magnetostriction coefficients. In the square-looped, polycrystalline ferrites I_s^2 is more than a factor of 100 smaller than in iron. This is apparently sufficient to satisfy Eq. (7′) even when there is no orientation of the axes of easy magnetization from grain to grain.

If the planar surface is a lamellar precipitate of

[4] C. Kittel, Revs. Modern Phys. **21**, 541 (1949).
[5] N. Menyuk and J. B. Goodenough, J. Appl. Phys. (to be published).

thickness d_l, then the demagnetization factor is 4π and

$$\sigma_0 = -\tfrac{1}{2}\int_0^{d_l} \mathbf{H}\cdot\mathbf{I}dz = 2\pi\omega_l^{*2}d_l.$$

Equation (7) then becomes

$$d_l\omega_l^{*2} < 10\sigma_w \approx 40[A(K+\lambda_i\sigma)]^{\frac{1}{2}}. \qquad (7'')$$

In metals this relationship is satisfied only if $d_l \approx 10^{-5}$ cm or less and in ferrites if $d_l \approx 10^{-4}$ cm or less. Materials in which extensive precipitation in lamellar sheets has occurred will have low remanence values.

C. The Crystal Surface

Every ferromagnetic lattice is bounded by its surface. If there were no internal defects to act as nucleating centers for a domain of reverse magnetization, the lattice would nevertheless not reverse its magnetization by a simultaneous rotation of all of its elementary magnetic moments unless it were so fine a particle that its diameter was the magnitude, or less, of a Bloch-wall thickness. Instead, a Bloch wall would enter from the surface of the crystal and move across the specimen. The crystal surface is another possible nucleating center for a domain of reverse magnetization. Both because the surface is irregular and because it is not, in general, parallel to a direction of easy magnetization in the adjacent grains, magnetic poles exist on the surface of the specimen even if it has a toroidal shape. These poles nucleate domains of reverse magnetization in a manner analogous to that of the grain boundary and lamellar precipitate. Since the surface pole density is large, however, H_w is generally large relative to H_c. The crystal surface is, therefore, an important source of mobile, 180° Bloch walls only if the H_n for the grain boundaries is larger than the H_w for the walls which are nucleated at the crystalline surface. In such cases the material usually exhibits a large Barkhausen discontinuity at $H=H_c$.

D. Summary

Of the lattice imperfections at which domains of reverse magnetization, and therefore 180° domain walls, might be created in a polycrystalline ferromagnetic, the grain boundary and, if present, the lamellar precipitate appear to be the most important. Small granular inclusions will not act as nucleating centers for domains of reverse magnetization. Larger inclusions may generate closure domains or, if there is but one axis of easy magnetization, domains of reverse magnetization, but these domains will be restricted to the region of the imperfection unless strong external magnetic fields are present. Similarly the domains associated with the magnetic poles on the surface of a specimen will be significant only if their H_w is smaller than the H_n and H_w for grain-boundary domains. The existence of closure or reverse domains, however, correspondingly reduces the retentivity of the specimen.

Since the nucleating field strength for reverse domains at grain boundaries is sensitive to the magnitude of the grain-boundary magnetic-pole strength $\omega^*=I_s(\cos\theta_1 - \cos\theta_2)$, the character of the B-H loop can be significantly altered by a variation of ω^* which changes $H_n<0$ to $H_n>0$. The magnitude of ω^* is frequently altered by magnetic anneal, grain orientation, or the application of tensile stress. In the next section it will be shown that the grain-boundary contribution to the coercive force is proportional to ω^{*2}/I_s. If this contribution is relatively large, a sufficient decrease in ω^* may make $H_n \geq H_c$ and therefore produce a square B-H loop.

III. THE COERCIVE FORCE

There are always several independent factors which contribute to the coercive force in any ferromagnetic material. If domain walls are present in a material, they are those factors which resist irreversible motion of these walls. In this paper four of these independent mechanisms will be discussed. They are the contributions to the total coercive force from granular inclusions, $H_w(\text{incl})$, grain boundaries, $H_w(\omega^*)$, lamellar precipitates, $H_w(\omega_l^*)$, and the surface tension in the expanding walls of a growing domain, $H_w(\sigma_w)$.

A. Granular Inclusions

Kersten[6] and Néel[7] have discussed the resistance to irreversible domain wall motion which is caused by inclusions that are free from associated closure domains. Williams and Shockley[8] have observed that when closure domains exist about inclusions, they retard 180° Bloch walls which move past them with a force proportional to their domain-wall surface tension. This mechanism is shown diagramatically in Fig. 4. If the inclusion resistance to irreversible motion of the 180° Bloch walls is due to the surface tension in the 90°

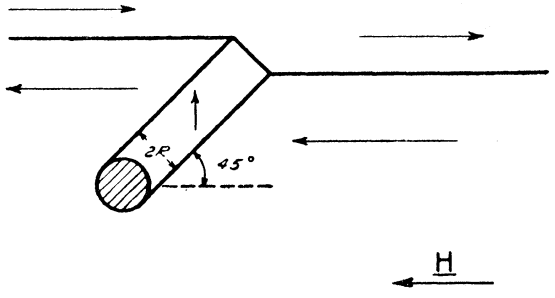

FIG. 4. The domain structure around an inclusion before the connection between the closure domain and the moving, 180° Bloch wall is broken.

[6] M. Kersten, *Grundlagen einer Theorie der Ferromagnetischen Hysterese und Koerzitivkraft* (S. Hirzel, Leipzig, 1943); Z. Physik **124**, 714 (1948).

[7] L. Néel, Cahiers phys. **25**, 21 (1944); Ann. univ. Grénoble **22**, 299 (1946); Physica **15**, 225 (1949); Bull. soc. franc. elec. [6] **9**, 308 (1949).

[8] H. J. Williams and W. Shockley, Phys. Rev. **75**, 178 (1949).

walls of the closure domains, then

$$2\mathbf{H}\cdot\mathbf{I}_s\Delta V=\sqrt{2}\pi R\sigma_w\Delta x,$$

where σ_w, the surface energy density of a 180° domain wall, is taken to be twice that for a 90° wall. If α is the angle between the applied field $\mathbf{H}$ and the spontaneous magnetization vector $\mathbf{I}_s$, if n is the average number of inclusions per cm² of 180° domain wall which have closure domains in contact with the moving wall, and if the average radius of the inclusions is $\langle R\rangle$, then

$$H_w(\text{incl})=(\pi/\sqrt{2}\cos\alpha)\cdot(\sigma_w/I_s)\langle R\rangle n.$$

If h is the mean distance between near-neighbor inclusions, $n\propto h^{-2}$. If P is the percentage of precipitate in the matrix, it is proportional to the ratio of the volumes of precipitate to total material, or to $\langle R\rangle^3/h^3$. Therefore $n\langle R\rangle=C_1P^{\frac{3}{2}}/\langle R\rangle$ and

$$H_w(\text{incl})=C_2(\sigma_w/I_s\langle R\rangle)P^{\frac{3}{2}}. \tag{8}$$

This mechanism cannot, of course, apply to those inclusions which are too small for closure domains to form about them.

B. Grain Boundaries and Lamellar Precipitates

1. If domains of reverse magnetization are created at planar surfaces of magnetic poles as indicated in Fig. 3, then the surface pole energy density which created the Bloch walls will resist their motion. If cylindrical domains of reverse magnetization are created at a planar surface with base radius r in elementary, periodic areas D^2, the energy associated with the surface magnetic poles is

$$\sigma=\sigma_0|\,(2\pi r^2/D^2)-1\,|+(\text{harmonic terms}).$$

At $H=H_w(\omega^*)$ the increase in energy associated with the surface magnetic poles must equal the decrease in energy resulting from the increased volume $\Delta V=\Delta[l_m\pi r^2(\cos\theta_1+\cos\theta_2)]$ which is aligned in the direction of H. $H_w(\omega^*)$ is the surface-pole-density contribution to the critical field strength for wall motion. The equilibrium relation $D^2\Delta\sigma=2\mathbf{H}_w(\omega^*)\cdot\mathbf{I}_s\Delta V$ then gives

$$H_w(\omega^*)=\left(\frac{D^2}{l_m}\right)\frac{d\sigma/d(r^2)}{2\pi I_sC_s}$$
$$\approx\frac{\sigma_0}{I_sl_mC_s}+\frac{1}{l_m}(\text{harmonic terms}), \tag{9}$$

where $C_s=(\cos\alpha_1\cos\theta_1+\cos\alpha_2\cos\theta_2)$. In zero approximation the contribution from the harmonic terms may be neglected.

If the planar surface is a grain boundary, $\sigma_0=(1/3)\pi\omega^{*2}L$ and $l_m=L$. Therefore, for small angles α_1, α_2, θ_1, and θ_2,

$$H_w(\omega^*)\approx\tfrac{1}{6}\pi I_s\langle(\cos\theta_1-\cos\theta_2)^2\rangle. \tag{9'}$$

Since $(\theta_1-\theta_2)\leq\pi/4$ in a lattice with three axes of easy magnetization, the grain-boundary contribution to the coercive force should be $H_w(\omega^*)\leq10^{-3}I_s$.

2. If the planar surface is a lamellar precipitate, its surface energy density is $\sigma_0=2\pi\omega_l^{*2}d_l$, and the percentage of foreign material present as precipitate is $P\propto$ (precipitate volume)/(volume of crystal). If, therefore, $2\alpha L^2$ is the principal surface area of parallel-oriented precipitate in a volume L^3, then

$$P\propto d_l\alpha L^2/L^3=d_l/l_m,$$

since the average distance between lamellar areas is $l_m=L/\alpha$. The contribution to the coercive force from the magnetic poles on the lamellar precipitate is, by Eq. (9), then

$$H_w(\omega_l^*)=C_3(\langle\omega_l^{*2}\rangle/I_s)P. \tag{9''}$$

The hypothesis of creation of domains of reverse magnetization at lamellar precipitates predicts, therefore, a linear increase in the coercivity with percent precipitate present.

C. Surface Tension

If domains of reverse magnetization are created as prolate ellipsoids of large eccentricity, the surface tension in the Bloch walls will resist domain growth. The force per unit area to contract a cylindrical wall of radius r and surface energy density σ_w is σ_w/r. The surface-tension contribution to the coercivity is therefore,

$$H_w(\sigma_w)=\sigma_w/2I_s\langle r_0\cos\theta\rangle \tag{10}$$

where $\langle r_0\rangle$ is the mean equilibrium radius of the newly created domains. If typical values $\langle r_0\rangle=\langle D/b\rangle\approx L/10$ and $L\approx5\times10^{-3}$ cm are chosen for a grain-boundary-nucleated domain,

$$H_w(\sigma_w)\approx10^3[\text{cm}^{-1}](\sigma_w/I_s)$$
$$\approx4\times10^3[\text{cm}^{-1}][A(K+\lambda_i\sigma)]^{\frac{1}{2}}/I_s. \tag{10'}$$

This term may be especially significant in square-looped ferrites in which (σ_w/I_s) is, by Eq. (7'), relatively large.

Further, it should be noted that $H_w(\text{incl})$ and $H_w(\sigma_w)$ are dependent directly upon the amount of internal strain present. This internal-strain dependence is in addition to that previously suggested[9,10] which is due to strain gradients in the material.

D. Temperature Dependence

Kersten[6] predicted, on the basis of his foreign-body theory of coercivity, a temperature dependence $H_c(T)\propto[K(T)]^{\frac{1}{2}}/I_s(T)$ for the coercivity of a strain-free material. The model of this paper predicts, for a strain-free material with no lamellar precipitates, a tempera-

[9] E. Kondorsky, Physik. Z. Sowjetunion 11, 597 (1937).
[10] M. Kersten, *Probleme der technischen Magnetizierungskurve*, edited by R. Becker (Julius Springer, Berlin, 1938); reprinted by J. W. Edwards, Ann Arbor.

ture dependence

$$H_c(T)=H_w(\sigma_w)+H_w(\text{incl})+H_w(\omega^*)$$
$$=a_1[AK(T)]^{\frac{1}{2}}/aI_s(T)+a_2I_s(T), \quad (11)$$

where a is the lattice parameter and a_1, a_2 are dimensionless, temperature-independent parameters given by

$$a_1=4a/\langle 2r_0\cos\theta\rangle+C_2P^{\frac{3}{2}}4a/\langle R\rangle\approx 10^{-4}+10^{-8}P^{\frac{3}{2}}\langle R\rangle,$$
$$a_2=\tfrac{1}{6}\pi\langle(\cos\theta_1-\cos\theta_2)^2\rangle$$
$$\approx 0.5\times 10^{-3} \text{ if no grain orientation.}$$

IV. CONCLUSIONS

A. Coercive Force and Starting Field

Of the four contributions to the coercive force which have been predicted in Sec. III, $H_w(\text{incl})$, $H_w(\omega_l^*)$, and $H_w(\omega^*)$ have been measured for typical cases. Measurements of H_c *vs* grain size are interpretable in terms of the fourth, $H_w(\sigma_w)$. The temperature-dependence of the coercive force in iron and nickel are available for comparison with Eq. (11).

1. In Fig. 5 are shown the measurements of Köster[11] on the change in coercivity with percent carbon in iron which is precipitated as lamellar and as granular cementite. The curved line is a graph of Eq. (8) with $C_2\sigma_w/I_s\langle R\rangle=6$, or $\langle R\rangle\approx 2\times 10^{-5}$ cm. This value of $\langle R\rangle$ is comparable with a critical radius for closure-domain formation. A $P^{\frac{3}{2}}$ law will prevail only so long as $\langle R\rangle$ does not vary appreciably with percent carbon content. For larger carbon content $\langle R\rangle$ should increase and H_c should fall below a strict $P^{\frac{3}{2}}$ plot. Such considerations indicate, therefore, that although the domains which are nucleated by inclusions will not grow away from them at low field strengths, they will offer a resistance to independent wall motion which is comparable to the coercive force of the material.

2. The straight line in Fig. 5 is $H_c=H_c'+12P$. The saturation magnetization of cementite is 1000 and of pure iron is 1700.[12] Therefore $\langle\omega_l^{*2}\rangle/I_s\approx 100$ oersteds. Since $C_3\approx 0.1$, Eq. (9″) not only predicts the straight-line relationship between H_c and P, but it also gives the correct order of magnitude for the slope of the line. This is to be contrasted with the granular-precipitate case which more nearly obeys a $P^{\frac{3}{2}}$ law.

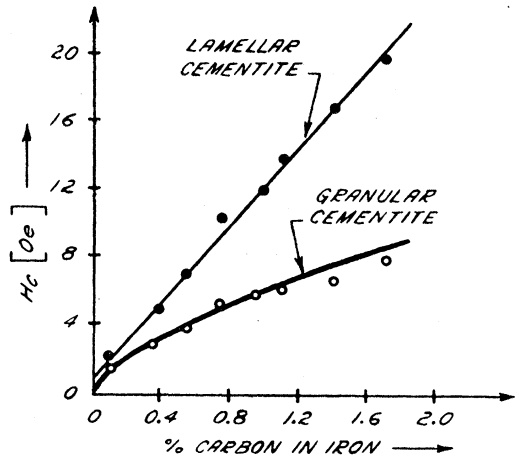

FIG. 5. The dependence of the coercive force, H_c, on the amount of carbon in iron in the form of granular and lamellar cementite (after Köster).

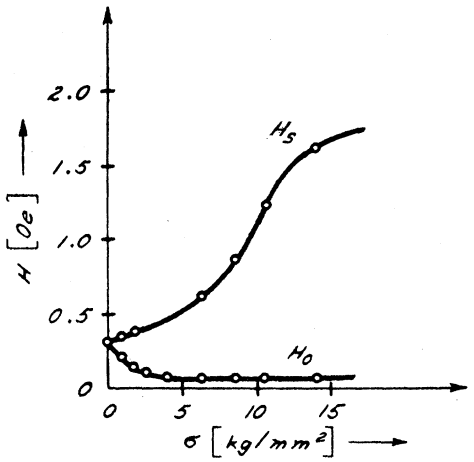

FIG. 6. The starting field, H_s, and the threshold field for domain-wall motion, H_0, *vs* applied tensile stress for a 78.5 Permalloy rod annealed 5 minutes at 800°C in vacuum (after Preisach).

3. Sixtus[13] and Preisach,[14] while studying the nucleation and propagation of domains of reverse magnetization in long wires of high-magnetostrictive-constant materials, observed the variation of H_s and H_0 with applied tensile stress σ on the wire. The starting field H_s represents the critical field strength necessary to initiate the single, large Barkhausen jump characteristic of this material. It corresponds to the nucleation field strength $H_n>H_c$. Since there is an alignment of the easy axis of magnetization by the applied tensile stress, $(\cos\theta_1-\cos\theta_2)$ decreases with increasing σ. Since $H_w(\omega^*)$ contributes to H_0, H_0 should decrease with σ according to Eq. (9′) whereas, by Eq. (7′), H_s should increase. In Fig. 6 are shown the measurements of Preisach on 78.5 Permalloy. These variations are as qualitatively predicted. The decrease in H_0 is nearly 0.3 oersted. This is the predicted order of magnitude for a partially grain oriented specimen. Sixtus has observed reductions in H_0 with applied tensile stress of as much as 6 oersteds. This corresponds to the maximum reductions predicted by Eq. (9′).

If the nucleation of the domain of reverse magnetization in these experiments is initiated at a grain boundary, as these figures strongly suggest, then the velocity of propagation of the reverse-magnetization zone as measured by a Sixtus-Tonks experiment will

[11] W. Köster, Arch. Eisenhüttenw. 4, 289 (1930).

[12] F. Stablein and K. Schroeter, Z. anorg. allgem. Chem. **174**, 193 (1938).

[13] K. J. Sixtus, *Probleme der Technischen Magnetizierungskurve* (Verlag Julius Springer, Berlin, 1938).

[14] F. Preisach, Physik. Z. **33**, 913 (1932).

be the velocity of the tip of the reverse-domain cone. If v is the normal velocity of the Bloch wall, the measured velocity will be v/λ. When this factor is taken into account, the Sixtus-Tonks measurements are in good agreement with the theoretical wall-velocity calculations and the direct measurements of wall velocity using colloidal magnetite techniques. It is also in agreement with the shape of the reverse-magnetization nucleus as observed by Sixtus[15] and by Ogawa.[16]

H_s may be expected to go through a maximum with increasing σ if the surface of the material rather than the grain boundary becomes the nucleation center at extremely small values of $(\cos\theta_1-\cos\theta_2)$.

4. Yensen and Ziegler[17] have measured the effect of grain size on the coercivity in iron. They found, for the grain-boundary contribution to the coercive force, $H_c[\text{oersteds}]=0.033\sqrt{N}\approx 3.7\times 10^{-3}/L[\text{cm}]$, where N is the number of grains per square millimeter and L is the mean grain diameter. Mager[18] postulated that one ellipsoidal domain of reverse magnetization is created at each grain boundary. He used Döring's[19] formulation for reverse-domain growth. He equated the average starting field for reverse-domain elongation with the observed H_c to obtain

$$H_c[\text{oersteds}]\approx\langle H_s\rangle=\frac{3}{2}\cdot\frac{3\pi\sigma_w}{4I_sL}\approx\frac{3.1\times 10^{-3}}{L[\text{cm}]}.$$

Mager is essentially calculating the contribution to the coercive force due to the surface tension of the 180° Bloch walls. Measurements[5] of flux-reversal times in magnetic cores as a function of the amplitude of a square-wave driving current indicate that the greatest distance a wall moves before the flux in a core is reversed is $\sim L$. However, the distance a wall moves before it collides with another is less than L. If more than one domain of reverse magnetization is created per average grain cross section, it is reasonable to take $\langle r_0\cos\theta\rangle \approx L/8$. Then Eq. (10) becomes

$$H_c[\text{oersteds}]=H_w(\sigma_w)\approx 4\sigma_w/I_sL=3.5\times 10^{-3}/L[\text{cm}].$$

This is a good order-of-magnitude agreement. The only other terms in the calculated contributions to the coercive force which vary as $1/L$ are the higher order terms in $H_w(\omega^*)$ [see Eq. (9)], and these are expected to be at least an order of magnitude smaller. Although Yensen and Ziegler's curve represents a mean of points with a certain amount of scatter, it is interesting to note that their measurements suggest that r_0 is proportional to L, or that roughly the same number of reverse domains are created per grain cross section over variations $10^{-2}\text{ cm}\leq L\leq 1\text{ cm}$.

5. In Fig. 7 are shown the temperature dependence in iron of the saturation magnetization and of $(AK)^{\frac{1}{2}}/aI_s$ as calculated by Kersten.[6] Kersten used Bozorth's[20] experimental values for the temperature dependence of the anisotropy constants of iron. In Fig. 8 are shown Kühlewein's[21] and Gans'[22] experimental coercivities of annealed iron as a function of temperature. The theoretical curve corresponds to Eq. (11) with $a_1=0.7\times 10^{-4}$ and $a_2=0.33\times 10^{-3}$. Both parameters a_1 and a_2 are of the correct order of magnitude. However, the entire magnitude of a_1 can be accounted for by the term $H_w(\sigma_w)$. Equation (11) reduces to Kersten's temperature-dependence formula if $a_2=0$, i.e., if the grain-boundary contribution to H_c is neglected. He shows a

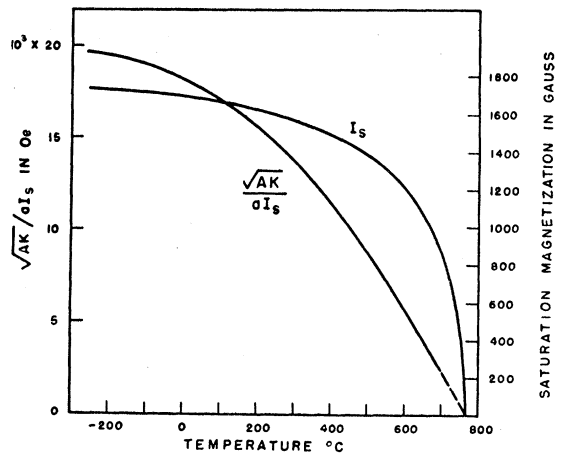

FIG. 7. Temperature dependence of the saturation magnetization I_s and the calculated temperature dependence of $(AK)^{\frac{1}{2}}/aI_s$ for iron where a is the lattice parameter, K the anisotropy constant, and $A=kT_c/a$ the exchange parameter (after Kersten).

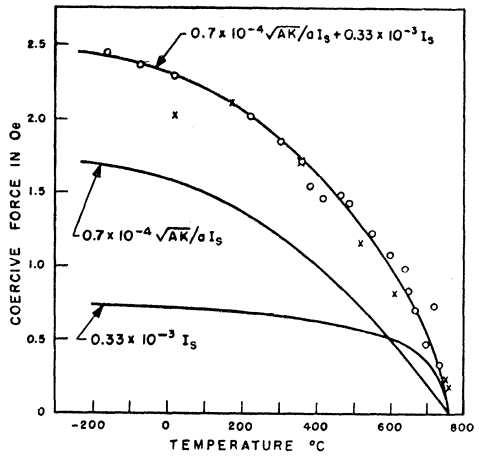

FIG. 8. Comparison of the experimental and theoretical temperature dependence of the coercivity in iron. Experimental points are ×, for "Swedish charcoal iron" after H. Kühlewein, and O, for "soft iron annealed at 800° C" after R. Gans.

[15] K. J. Sixtus, Phys. Rev. **48**, 425 (1935).
[16] S. Ogawa, Science Repts. Research Insts. Tôhoku Univ. Ser. A, **1**, 53 (1949).
[17] T. D. Yensen and N. A. Ziegler, Trans. Am. Soc. Metals **23**, 556 (1935).
[18] A. Mager, Ann. Physik **11**, 15 (1952).
[19] W. Döring, Z. Physik **108**, 137 (1938).
[20] R. M. Bozorth, J. Appl. Phys. **8**, 575 (1937).
[21] H. Kühlewein, Wiss. Veröffentl. Siemens-Werke **11**, 126 (1932).
[22] R. Gans, Ann. Physik **48**, 514 (1915).

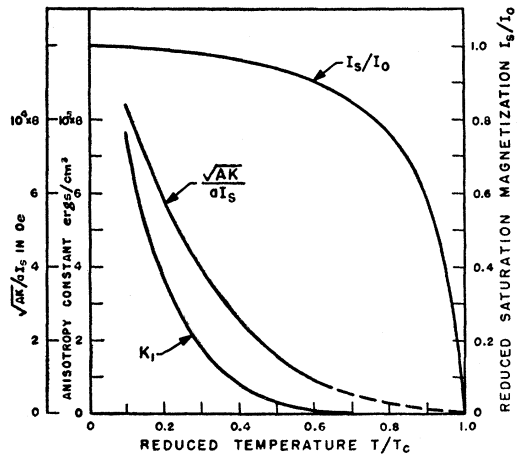

FIG. 9. Calculation of $(AK)^{\frac{1}{2}}/aI_s$ for nickel, where a is the lattice parameter and $A=kT_c/a$ is the exchange parameter. The curves for the anisotropy constant K and the reduced saturation magnetization I_s/I_0 are taken from R. Becker and W. Döring, *Ferromagnetismus* (Julius Springer, Berlin, 1939; reprinted by J. W. Edwards, Ann. Arbor, Figs. 78 and 25.

best-fit for the experimental data with $a_1=1.05\times10^{-4}$, but his curve does not follow the data nearly as well as that shown in Fig. 7. There can be no doubt that the grain-boundary contribution to the coercivity cannot be neglected in this case.

Gerlach[23] has measured the coercivity of nickel as a function of the temperature (Fig. 9). He sintered nickel-carbonyl powder in a quartz tube at 1000°C for 1 to 2 hours. The sample was a long, thin rod of density roughly 98 percent that of crystallized nickel. In Fig. 10 is shown a comparison of the experimental coercivities with the theoretical H_c *vs* T curve for $a_1=0.96\times10^{-4}$ or 1.14×10^{-4} and $a_2=0.33\times10^{-3}$. In the case of nickel the grain-boundary contribution to the coercivity is much smaller than the other terms because of the relatively low value of I_s. For this reason Gerlach assumed that the relation $H_c(T)\propto[K(T)]^{\frac{1}{2}}/I_s(T)$ was proven sufficient to explain the experimental results. It should be noted that again a_1 and a_2 are the orders of magnitude predicted by Eq. (11).

There can be no doubt that the predominant contribution to the coercivity in the nickel sample varies as $K^{\frac{1}{2}}/I_s$. This indicates that whatever contribution to the coercive force arises from inclusions which are too small to have closure domains associated with them is either small or also varies as $K^{\frac{1}{2}}/I_s$. Néel's[7] model predicts a temperature variation $[0.386+\log(2\pi I_s^2/K)^{\frac{1}{2}}]K/I_s$. Kersten's[6] model predicts a temperature dependence proportional to $K^{\frac{1}{2}}/I_s$, but this model is open to the criticism that an assumed periodic distribution of the inclusions leads to too high a coercive-force contribution. If the inclusions are randomly distributed through the lattice, the number of inclusion per unit area of wall which are intersected by a 180° Bloch wall should be roughly constant for various wall positions. Since the contributions $H_w(\sigma_w)$ and $H_w(\text{incl})$ of this paper are sufficient to account for the magnitude of the coercivity, there is no need to invoke an artificially periodic inclusion distribution. The contribution to the coercivity from inclusions which are too small to cause closure-domain formation may indeed be a minor one.

[23] W. Gerlach, Z. Physik **133**, 286 (1952).

B. Stress Hysteresis

Since the work of Ewing[24] before the turn of the century, stress hysteresis in ferromagnetic materials at constant field strengths has been observed, but no satisfactory explanation of this phenomenon has been offered. The hypothesis of nucleation at grain boundaries, however, provides a simple, qualitative understanding of the complex phenomenon. Besides rotation of the spontaneous magnetization vectors in an applied field, there are two principal mechanisms which are responsible for flux change in a magnetic material, *viz.*, domain creation and Bloch-wall movement. Each of these may be either reversible or irreversible. The hypothesis of nucleation at grain boundaries predicts, through Eqs. (7′) and (9′), that in an external field H the change of an applied stress which alters ω^* will have two important effects. First, if ω^* is decreased until $H_w(\omega^*)<H$, an existing domain will grow or

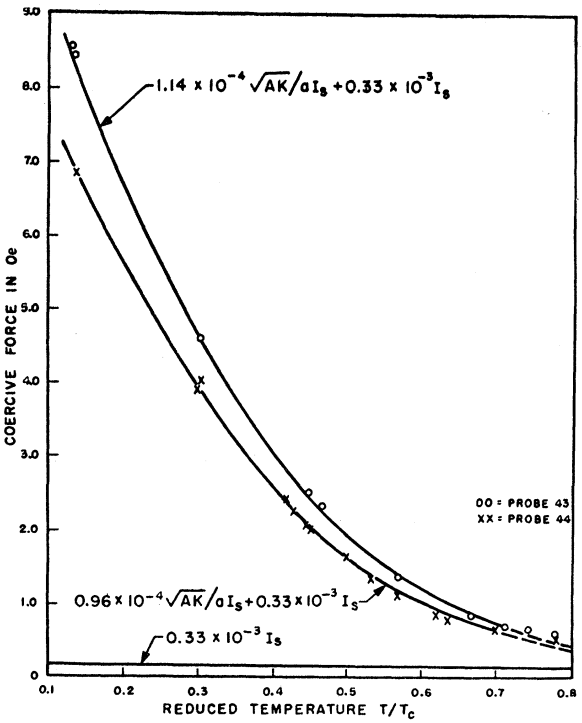

FIG. 10. Comparison of the experimental and theoretical temperature dependence of the coercivity in nickel. Experimental points after W. Gerlach.

[24] J. A. Ewing, *Magnetic Induction in Iron and Other Metals* ("The Electrician" Printing and Publishing Company, London, 1900), third edition.

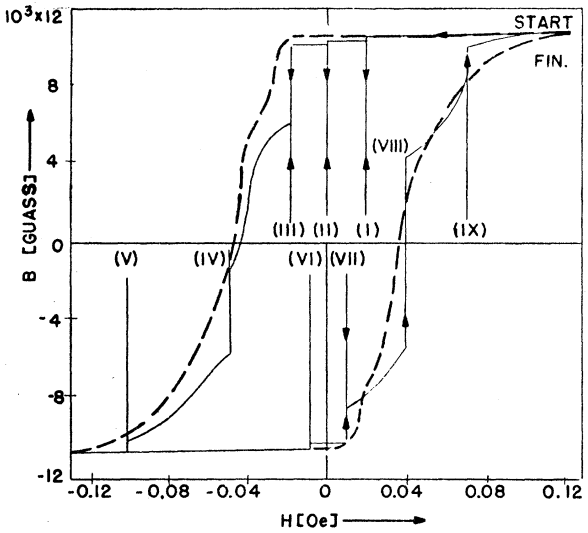

FIG. 11. Hysteresis loop of 68 Permalloy under tension of 4 kg/mm² except when stress removed and reapplied at certain field strengths (after Bozorth).

contract according to its orientation with respect to H. Second, the number of nucleated domains present at a given H will vary with the value of ω^*. If a decrease in ω^* makes $H_n > H$, the surface tensions in the Bloch walls will exceed the net force to maintain domains of reverse magnetization which are nucleated at grain boundaries. There results a net force to shrink such a domain to zero volume. Of the several experiments described by Bozorth in Chapter 13 of *Ferromagnetism* which could be chosen to illustrate this hypothesis, two will be discussed in detail here.

(1) Figure 11 shows a B-H loop of 68 Permalloy[25] which was taken with a stress $\sigma = 4$ kg/mm² continually maintained (broken line) and a loop (solid line) with the same stress released and then reapplied at various constant values of H marked (I)–(IX). In 68 Permalloy $\sigma_w/I_s^2 \approx 10^{-7}$ cm. If the mean grain size is assumed to have been $L = 5\times10^{-3}$ cm, Eq. (7′) becomes $(\cos\theta_1 - \cos\theta_2)^2 < 10^{-3}$ or $(\theta_1 - \theta_2) < 15°$. Therefore one may expect $H_n < 0$ if there is no orientation of the axis of easy magnetization from grain to grain. Application of $\sigma = 4$ kg/mm², however, is sufficient to align the axes of easy magnetization in the direction of the applied tensile stress. The low value of K in this material makes its direction of easy magnetization particularly sensitive to a tensile stress. If $(\theta_1 - \theta_2) \ll 15°$, Eq. (7′) gives $H_n > 0$ and $H_w(\omega^*)$ is small. The factors affecting Fig. 11 may therefore be qualitatively understood as follows.

When the stress is released at (I), the direction of easy magnetization is no longer aligned by the stress. The spontaneous magnetization vectors of the individual grains rotate to a set of axes which are determined by the crystallographic orientation of the grains. The contribution to the flux change due to this rotation is reversible and small compared to the observed flux change of nearly a factor of six. The change of flux due to such rotations will not be mentioned in the subsequent discussion. It will be understood that this contribution is always present. The significant feature is that ω^* increases when the stress is removed. This increase is sufficient, apparently, to make $H_n < H(\text{I})$. There results a nucleation of many domains of reverse magnetization at the grain boundaries with a resultant large decrease in the induction through the sample. When σ is reapplied, ω^* decreases again to make $H_n > H(\text{I})$. Since $H(\text{I})$ is opposed to the formation of reverse domains, the domains which were created when σ was released disappear when σ is reapplied. There are a few domains which are irreversibly created, however, so that the induction through the sample is not completely regained by the reapplication of σ.

At (II) and (III) the process is the same as at (I) except that more domains of reverse magnetization are irreversibly created. The field $H(\text{III})$ opposes the Bloch-wall-surface-tension forces which are acting to destroy the new domains when the stress is reapplied.

At (IV) there is, initially, a large percentage of the specimen's volume within domains antiparallel as well as parallel to $H(\text{IV})$. When σ is released, the increase in ω^* is sufficient to create new domains. These are oriented parallel or antiparallel to $H(\text{IV})$ depending upon the orientation of the larger domain in which they are formed. Since a larger volume of material is oriented parallel than antiparallel to $H(\text{IV})$, more new domains are oriented antiparallel to $H(\text{IV})$ and the induction decreases slightly. When σ is reapplied, however, the domains which were created antiparallel to $H(\text{IV})$ disappear whereas those created parallel to $H(\text{IV})$ remain and even grow. The marked increase in $|B|$ results.

The mechanisms at (V) and (IX) are the same as at (IV) except that the proportion of created domains which are oriented parallel to H is greatly reduced. The mechanisms at (VI) and (VII) are the same as those at (I), (II), and (III).

When σ is released and ω^* increases at (VIII), the majority of new domains are oriented parallel to $H(\text{VIII})$. A sharp decrease in $|B|$ results. Since $H(\text{VIII}) \approx H_c(\sigma = 4$ kg/mm²), the favorably oriented domains grow while the unfavorably oriented ones disappear when σ is reapplied. Consequently the induction continues to decrease until it changes sign and increases in the opposite direction.

Completely analogous reasoning can account for the B-H loop[25] taken with no stress applied except at certain values of H at which it is applied and subsequently released.

(2) Figure 12[25] shows the effects on the initial magnetization curve for 68 Permalloy of applying the tensile stress σ and the magnetization field H in different

[25] R. M. Bozorth, *Ferromagnetism* (D. Van Nostrand Company, Inc., New York, 1951), Chap. 13.

orders. Curve (a) is the normal initial-magnetization curve. Since ω^* is large, $H_w(\omega^*)$ is large. For $H<0.1$ oersted, therefore, there is little Bloch-wall motion, and the permeability remains low. When $\sigma=4$ kg/mm^2 is applied, the term $H_w(\omega^*)$ is reduced, and the total coercivity is lowered to $H_c=0.042$ oersted. At $H=0.1$ oersted on curve (b), therefore, most of the domain-wall motion has taken place. Since the spontaneous-magnetization vectors are largely aligned by the stress and the wall motion is nearly completed, the induction has already increased to nearly its saturation value at $H=0.1$ oersted.

If a field H is applied prior to σ, a force will exist to shrink those domains which are aligned antiparallel to H which is the sum of that due to the field and that due to the surface tensions in the Bloch walls. Even at field strengths $H<H_c(\sigma=4$ kg/mm$^2)$, this sum will be sufficient to collapse many domains which are antiparallel to H if $H_w(\omega^*)$ is reduced by the application of σ. The initial permeability for curve (d) is, therefore, extremely large. Domain-wall surface tensions in excess of tension equilibrium do not exist if the material is demagnetized under a tensile load and then magnetized without removing the stress, as in curve (b).

If the stress is applied and then released after the field H has been applied, the initial magnetization curve traces out the curve (c). When the stress is released, the magnetization drops from curve (d) to curve (c) because of the nucleation of domains of reverse magnetization within the large domains oriented parallel to H. The initial permeability is high because the domains which are nucleated when σ is released occupy considerably less than half the volume whereas the original domains oriented antiparallel to H occupied, from curve (a), nearly half the total volume of the specimen.

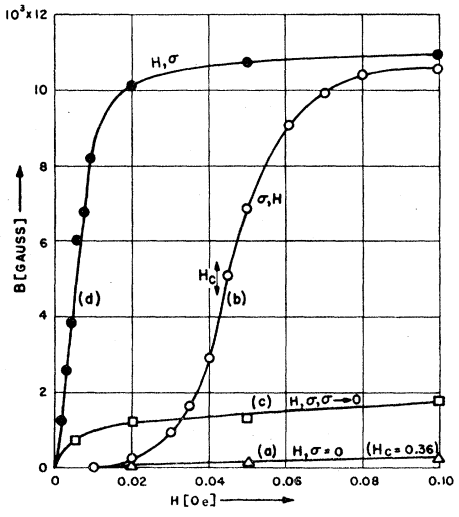

FIG. 12. Various kinds of initial magnetization curves of 68 Permalloy: (a) Normal curve with no tension. (b) $\sigma=4$ kg/mm^2 applied first, and then the external field H. (c) H applied, σ applied and removed several times. (d) H applied first, and then σ (after Bozorth).

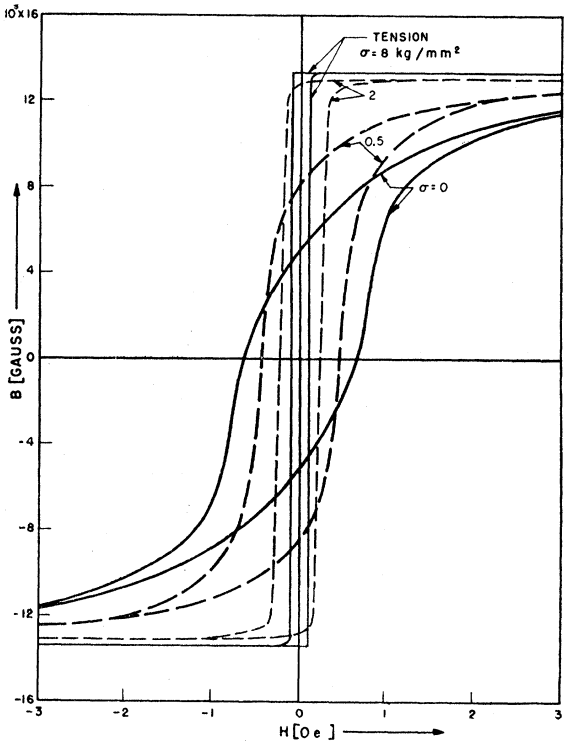

FIG. 13. Hysteresis loops of 68 Permalloy under various tensions σ. Maximum field strength 5 oersteds (after Bozorth).

C. *B-H* Loop Shape

If nucleation of domains of reverse magnetization occurs at the grain boundary with an $H_n<0$, the B-H loop shape will be profoundly affected by a decrease in ω^* which makes $H_n>0$. This is usually accomplished in metals by a reduction in $(\cos\theta_1-\cos\theta_2)$ through grain orientation, magnetic anneal, or application of a tensile stress. Figure 13[25] shows the effect of applying a tensile stress to 68 Permalloy. H_n is seen to increase with stress whereas H_c decreases some 0.6 oersted. This is in complete agreement with Eqs. (7′) and (9′).

In the ferrites the available methods for reducing $(\cos\theta_1-\cos\theta_2)$ are more limited. Williams[26] has recently squared the B-H loop of a nickel-zinc ferrite by the application of a compressive stress. Since the magnetostrictive coefficient is negative in this material, this behavior is analogous to that found in 68 Permalloy under a tensile stress. The increase in H_c with $\sigma>0.65$ kg/mm^2 is attributed $H_c=H_n>H_w$. It should also be realized that the application of σ increases the amount of internal strain present in the material. The internal-strain contribution to σ_w should increase the coercive force with an increase of σ. The surprising fact that in some metal specimens H_c decreases with σ is attributed

[26] Williams, Sherwood, Goertz, and Schnettler, Communications and Electronics No. 9, 531 (1953).

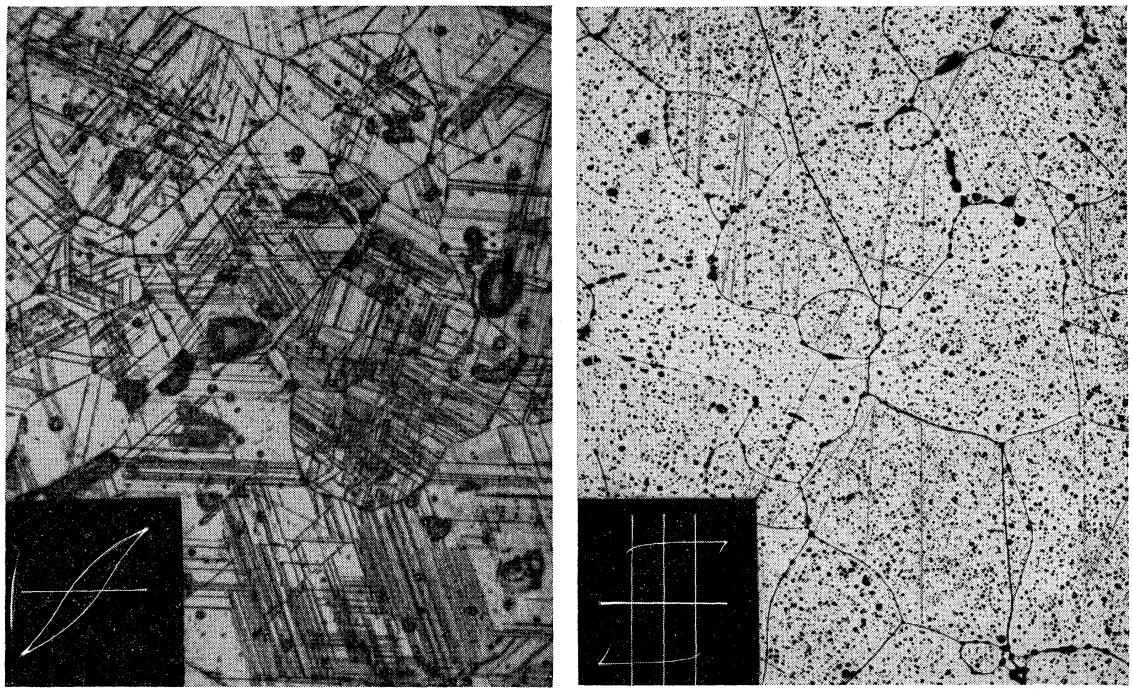

(a) (b)

FIG. 14. Microstructure and maximum-squareness-ratio B-H loop for a General Ceramics Company MF-1371-B ferrite body (a) before anneal (white light×498, $B_m=150$ gauss, $H_m=2.25$ oersteds) and (b) after anneal (white light×100, $B_m=1128$ gauss, $H_m=0.46$ oersted).

to a predominance of $H_w(\omega^*)$ in the coercivity of these materials. In the ferrites $H_w(\omega^*)\lesssim 0.1$ oersted is usually a small fraction of H_c.

An alternative approach to attain a material with a square B-H loop is to reduce I_s and to increase $\sigma_w \propto [A(K+\lambda_i\sigma)]^{\frac{1}{2}}$. Square-looped materials have correspondingly been obtained in magnesium and in magnesium-manganese ferrites. The magnesium ferrite has a low I_s. The addition of manganese is believed to introduce internal strains e which increase the effective anisotropy constant $(K+\lambda_i Ee)$, where E is Young's modulus.

D. Micrograph Studies

If nucleation of domains of reverse magnetization occurs at grain boundaries, the corresponding Bitter patterns on polished surfaces parallel to a direction of easy magnetization should show triangles with their base at a grain boundary. Such patterns have been observed by Williams in silicon iron.[4] Fowler and Fryer[27] have observed the predicted nucleation and growth of domains of reverse magnetization from the surface (rather than a grain boundary) of a single crystal of silicon iron. Martin[28] has observed the creation and growth of dagger-shaped closure domains at lattice imperfections and the crystal surface in a single crystal of 3 percent silicon iron which was rotated from an easy axis of magnetization in an external field.

In Fig. 14 is shown[29] a photograph of the microstructure in a General Ceramics and Steatite Corporation MF-1371B ferrite body before and after an anneal. The preannealed sample is heavily twinned. Precipitation has occurred at the twinning surfaces. There results a lamellar precipitate along certain crystallographic planes. (The dark spots, or blobs, correspond to voids in the lattice.) This material had a nonsquare loop. It showed the characteristics of a sample with $H_n<0$. It is proposed that nucleation takes place at the lamellar precipitate because the condition of Eq. (7″) is not fulfilled. The coercive force is relatively large through the precipitate contribution of Eq. (9″). During anneal the Widmanstätten structure disappeared. The B-H loop became extremely square. This is understandable on the basis that though $H_n<0$ for the lamellar precipitate, for the grain boundary $H_n>0$. It is to be expected that $\omega_l{}^*>\omega^*$.

It should also be noted that the Widmanstätten lines indicated no grain orientation in the material. As there has been no magnetic anneal and there are no apparent microscopic stresses which could align the directions of easy magnetization away from preferred

[27] C. A. Fowler and E. M. Fryer, Revs. Modern Phys. **25**, 33 (1953).

[28] D. H. Martin, Proc. Phys. Soc. (London) **B66**, 712 (1953).

[29] S. Andrew Kulin, Lincoln Laboratory, Massachusetts Institute of Technology (unpublished research).

crystallographic directions, the squareness of the B-H loop of the annealed sample is not attributed to a low value of $(\cos\theta_1-\cos\theta_2)$. It is rather attributed to a relatively low ratio I_s^2/σ_w.

ACKNOWLEDGMENT

The author would like to express his thanks to R. M. Bozorth of the Bell Telephone Laboratories and to his publishers, the D. Van Nostrand Company, Inc., for permission to reprint Figs. 11, 12, and 13 from Chapter 13 of *Ferromagnetism* (copyrighted 1951). He would also like to thank N. Menyuk for his lively interest in the work and for checking the arithmetic calculations.

APPENDIX I

The energy associated with a small, spherical inclusion imbedded in a material of spontaneous magnetization I_s is given by its demagnetization energy

$$-\tfrac{1}{2}\int \mathbf{H}\cdot\mathbf{I}_s dV=(8\pi^2/9)I_s^2R^3. \qquad (I.1)$$

The critical radius, at absolute zero of temperature, is that for which this energy just equals the energy of the configuration with closure domains present. Since the closure domain essentially eliminates the magnetic poles at the inclusion surface,

$$(8\pi^2/9)I_s^2R_c^3=\tfrac{1}{2}\sigma_w A_w+E_d+E_{el}, \qquad (I.2)$$

where σ_w, the energy per unit area of a 180° wall, is taken as twice that for a 90° wall. A_w is the area of 90° wall which bounds the closure domains. E_d is the demagnetization energy of the closure domain, and E_{el} is the elastic energy associated with the closure domain as a result of the magnetostriction. For simplicity, the closure domain may be considered a prolate ellipsoid whose ratio of semiminor to semimajor axes is $\lambda=R_c/\sqrt{2}l\ll 1$. The demagnetization energy and Bloch-wall area are then

$$E_d=(4\pi^2\eta/3\sqrt{2})\lambda[\ln(2/\lambda)-1]I_s^2R_c^3, \quad A_w=\pi^2R_c^2/2\lambda,$$

where η is a numerical factor which takes account of the permeability of the matrix.[30]

The conventional first-order magnetostriction equation is given by Becker and Döring[31] as

$$e=\delta l/l=\tfrac{3}{2}\lambda_{100}(\alpha_1^2\beta_1^2+\alpha_2^2\beta_2^2+\alpha_3^2\beta_3^2-\tfrac{1}{3})+3\lambda_{111}(\alpha_1\alpha_2\beta_1\beta_2+\alpha_1\alpha_3\beta_1\beta_3+\alpha_2\alpha_3\beta_2\beta_3),$$

where $\boldsymbol{\alpha}=(\alpha_1,\alpha_2,\alpha_3)$ is a unit vector in the direction of the magnetization, $\boldsymbol{\beta}=(\beta_1,\beta_2,\beta_3)$ is a unit vector in the direction in which the strain e is measured; λ_{100} and λ_{111} are the saturation values of the longitudinal magnetostriction in the directions [100] and [111], respectively. The elastic energy density in a cubic crystal is given by[32]

$$f_{el}=\tfrac{1}{2}c_{11}(e_{xx}^2+e_{yy}^2+e_{zz})+\tfrac{1}{2}c_{44}(e_{xy}^2+e_{yz}^2+e_{zx}^2)+c_{12}(e_{yy}e_{zz}+e_{xx}e_{zz}+e_{xx}e_{yy})$$

where the c_{ij} are the elastic moduli and the e_{ij} are strains as defined by Love.[32] To estimate the elastic energy E_{el}, it is assumed that the lattice outside the closure domain is not distorted. If the [100] direction is an axis of easy magnetization, $f_{el}=\tfrac{1}{2}c_{11}\lambda_{100}^2$ and

$$E_{el}=(\pi/3\sqrt{2}\lambda)R_c^3c_{11}\lambda_{100}^2.$$

If the [111] direction is an axis of easy magnetization, $e=\tfrac{1}{4}\lambda_{100}+\tfrac{3}{2}\lambda_{111}$ and $f_{el}=\tfrac{1}{2}(c_{11}+c_{12})e^2$ so that

$$E_{el}=(\pi/3\sqrt{2}\lambda)R_c^3(c_{11}+c_{12})(\tfrac{1}{4}\lambda_{100}+\tfrac{3}{2}\lambda_{111})^2.$$

Equation (I.2) therefore gives

$$R_c=f(\lambda)\cdot(\sigma_w/I_s^2);$$
$$f(\lambda)=9/\{32\lambda-C-24\sqrt{2}\lambda^2\eta[\ln(2/\lambda)-1]\},$$

where

$$C=(6\sqrt{2}/\pi I_s^2)C';$$

$$C'=\begin{cases}c_{11}\lambda_{100}^2 & \text{if magnetization along [100]}\\ (c_{11}+c_{12})(\tfrac{1}{4}\lambda_{100}+\tfrac{3}{2}\lambda_{111})^2 & \text{if magnetization along [111].}\end{cases}$$

The colloidal-magnetite patterns of Williams[2] show a $\lambda\approx 1/30$. In iron[4] $C\approx 5\times 10^{-3}$ and $(\sigma_w/I_s^2)\approx 10^{-6}$ cm so that $R_c\approx 10^{-5}$ cm.

APPENDIX II

The field strength, at absolute zero, which is required to rotate a closure domain through an angle θ_1 is given by

$$H\left\{\int_0^{\theta_1}\int_{-l(\theta)}^{l(\theta)}\rho_l^*(x,\theta)x\sin\left(\frac{\pi}{4}-\theta\right)dxd\theta+I_sV\sin 2\theta_1\right\}+\Delta E_{el}=\tfrac{1}{4}VK\sin^2 4\theta_1+\Delta E_d+\Delta(\sigma_w A_w),$$

where K is the anisotropy constant. $V=(4\pi/3\lambda)a^3\cos^3\theta_1$ is the volume of the domain after rotation through θ_1. The ratio of the semiminor to semimajor axes of the original closure domain, $\lambda=a/l$, is assumed to remain constant. The torque exerted by the interaction of the external field with the Bloch-wall magnetic poles is taken as the torque the field would exert on the closure-domain axis if it contained an equivalent linear pole density ρ_l^*. If the equation of the closure-domain ellipsoid is taken as

$$F(x,y,z)=\frac{x^2}{l^2}+\frac{y^2+z^2}{r^2}-1=0,$$

[30] Williams, Bozorth, and Shockley, Phys. Rev. **75**, 155 (1949).

[31] R. Becker and W. Döring, *Ferromagnetismus* (Julius Springer, Berlin, 1939; reprinted J. W. Edwards, Ann Arbor).

[32] A. E. H. Love, *A Treatise on the Mathematical Theory of Elasticity* (Cambridge University Press, Cambridge, 1927), fourth edition, p. 38.

the surface pole density is

$$\omega_d^* = \eta(1+\sin 2\theta) I_s F_x / |\nabla F|.$$

The equivalent linear pole density is

$$\rho_l^*(x,\theta) = \omega_d^* 2\pi y |\nabla F| / F_y = 2\pi(1+\sin 2\theta)\eta I_s \lambda^2 x.$$

The change in demagnetization energy is

$$\Delta E_d = (8\pi^2\eta/3) I_s^2 \lambda [\ln(2/\lambda) - 1] \times a^3 \{(1+\sin 2\theta_1)^2 \cos^3\theta_1 - 1\},$$

and the change in wall energy is

$$\Delta(\sigma_w A_w) = \frac{\pi^2 a^2}{\lambda} \sigma_w \left\{ \frac{\sigma_w(\theta_1)}{\sigma_w} \cos^2\theta_1 - 1 \right\}.$$

Although the volume of material completely within the closure domain decreases as it is rotated to form a domain of reverse magnetization, the Bloch walls are increasing in thickness. It is assumed that the change in volume is absorbed in this greater wall thickness. As the wall thickness increases, the surface wall-energy density increases from σ_w to $\sigma_w(\theta_1)$. The change in total elastic energy due to rotation through θ_1 is given approximately by

$$\Delta E_{el} = (2\pi a^3/3\lambda) C' (1 - \cos 2\theta_1).$$

This elastic energy is relieved when the closure domain is rotated to become a domain of reverse magnetization.

If the magnetic anisotropy of the crystal offers the greatest resistance to rotation of the closure domain in the external field, then the minimum field strength in which a domain of reverse magnetization can be created is that which rotates the domain $\pi/8$ radians. If $\theta_1 = \pi/8$, $\eta = 0.1$, and $\lambda = 1/30$, then

$$H_n \approx \frac{1}{3}\frac{K}{I_s} + 0.004 I_s + \frac{5}{2}\frac{\sigma_w}{R I_s} - \frac{1}{4}\frac{C'}{I_s},$$

where R is the mean radius of the inclusion.

APPENDIX III

In order to calculate H_w for a domain of reverse magnetization at a spherical inclusion, it is assumed that the inner domain of Fig. 2(b) forms with a semiminor axis $r_1 = R_c/\sqrt{2}$. The critical radius R_c is the smallest radius a spherical inclusion can have and nucleate a domain of reverse magnetization in zero external field. Both domains are assumed to be prolate ellipsoids of revolution. The ratio of semiminor to semimajor axes λ is taken to be the same for both domains and to remain constant as the domains grow. The critical radius, at absolute zero of temperature, is that for which the demagnetization energy of Eq. (I.1) just equals the energy of the configuration with a domain of reverse magnetization present. Since the energy of the new polar configuration about the inclusion will be to the old as a quadruple term to a dipole term, it can, to a first approximation, be neglected and

$$(8\pi^2/9) I_s^2 R_c^3 = \sigma_w A_w + E_d. \qquad \text{(III.1)}$$

Since $\lambda \ll 1$ and $r_1 = R_c/\sqrt{2}$, the demagnetization energy is

$$E_d = \frac{16\pi^2\eta}{3\sqrt{2}} \left[\ln\left(\frac{2}{\lambda}\right) - 1 \right] \lambda I_s^2 R_c^3,$$

and the area of 180° Bloch wall is

$$A_w = \pi^2 R_c^2 / 2\lambda.$$

Equation (III.1) therefore gives

$$r_1 = R_c/\sqrt{2} = F(\eta,\lambda)\sigma_w / I_s^2;$$

$$F(\eta,\lambda) = \frac{9/16\lambda}{\sqrt{2} - \eta 6\lambda[\ln(2/\lambda) - 1]}.$$

If ΔV is the increase in the volume of material magnetized parallel to the external field and if the interaction energies between the Bloch-wall poles of the two domains and between them and the inclusion-surface poles are E_{np} and E_p, then H_w, at absolute zero of temperature, can be derived from the energy balance

$$2 I_s H_w \Delta V = \Delta(\sigma_w A_w) + \Delta E_p + \Delta E_d + E_{np}. \qquad \text{(III.2)}$$

The change in energy associated with the interaction of the inclusion-surface poles is negligible compared to the other terms.

Let $r_0 = R/\sqrt{2}$ be the minor axis of the first nucleated domain when there is no field present and r_2 be its value at $H = H_w$, the field strength at which the second domain of minor axis r_1 is nucleated within it. Then $r_2^2 = r_1^2 + R^2/2$ and, provided $r_1/R \ll 1$,

$$\Delta V \approx \frac{\pi}{\lambda} r_1^2 R \left\{ \sqrt{2} - \frac{4}{3}\left(\frac{r_1}{R}\right) \right\},$$

$$\Delta(\sigma_w A_w) = \frac{2\pi^2 I_s^2}{\lambda F(\eta\lambda)} r_1^3, \qquad \text{(III.3)}$$

$$\Delta E_d = 8\pi^2\eta \left[\ln\left(\frac{2}{\lambda}\right) - 1 \right] I_s^2 \lambda r_1^2 R \left\{ \sqrt{2} + \frac{4}{3}\left(\frac{r_1}{R}\right) \right\}.$$

Since $\lambda \ll 1$, it is possible to estimate E_p by assuming the Bloch-wall poles are equivalent to an axial linear pole density $\rho_l^* = 4\pi I_s \eta \lambda^2 x$. Since the inclusion-surface poles are equivalent to a plane with concentric circles circumscribing regions of uniform surface pole density $\pm I_s$,

$$\frac{1}{2}\Delta E_p = \frac{1}{2}\int_0^{l_1} \int_S \frac{\omega^*(2) dS \rho_l^* dx}{(x^2+r^2)^{\frac{1}{2}}} + \frac{1}{2}\int_0^{l_2} \int_S \frac{\omega^*(2) dS \rho_l^* dx}{(x^2+r^2)^{\frac{1}{2}}} - \frac{1}{2}\int_0^{l} \int_S \frac{\omega^*(1) dS \rho_l^* dx}{(x^2+r^2)^{\frac{1}{2}}},$$

where

$$\omega^*(2)=\begin{cases} I_s \text{ for} \begin{cases} 0\le r\le r_1 \\ r_2\le r\le R \end{cases} \\ -I_s \text{ for } r_1\le r\le r_2, \end{cases}$$

$$\omega^*(1)=\begin{cases} -I_s \text{ for } 0\le r\le r_0 \\ I_s \text{ for } r_0\le r\le R. \end{cases}$$

Integration yields

$$\Delta E_p=f_p(\lambda, r_1/R)I_s^2R^3. \qquad \text{(III.4)}$$

If the inner-domain-Bloch-wall poles are approximated by the axial linear pole density ρ_l^*, then

$$\frac{1}{2}E_{np}=\frac{1}{2}\int_{S_2}\int_0^{l_1}\frac{\rho_{l1}^*dx_1\omega_2^*dS_2}{[(x_1-x_2)^2+\lambda^2(l_2^2-x_2^2)]^{\frac{1}{2}}},$$

where $\omega_2^*dS_2=4\pi\eta I_s\lambda^2x_2dx_2$. Since $\lambda\ll1$, this gives

$$E_{np}=f_{np}(\lambda, r_1/R)I_s^2r_1^2R. \qquad \text{(III.5)}$$

If Eqs. (III.3), (III.4), and (III.5) are substituted into (III.2), there results

$$H_w=I_s\left\{Q_1(\eta,\lambda)+\frac{R_c}{R}Q_2(\eta,\lambda)+\cdots\right\}.$$

If the values $\lambda=1/30$, $\eta=0.1$ are taken, Eq. (3) results.

APPENDIX IV

To estimate the various terms in ΔF [see Eq. (5)], several simplifying assumptions are made. Obviously σ_0 is independent of r, and σ_n can be calculated as outlined by Kittel.[4] Thus $\sigma_n=f(b)\omega^{*2}D$, where $f(b)$ is a term of the order of unity which depends upon $b=D/r$.

Since $\lambda\ll1$ and $r<D$, the Bloch-wall poles are assumed equivalent to an axial pole density $\rho_l^*=4\pi I_s\lambda^2x$. To estimate E_p, it is further assumed that this axial pole density is perpendicular to the grain boundary and that the first zone of positive and negative grain-boundary-surface poles at its foot gives the major contribution to E_p. Then if r' is the radius vector from the foot of the major axis in the grain-boundary plane and $b\lambda\ll1$,

$$E_p\approx\pi\int_{r'}\int_{-l}^{l}\frac{\omega^*r'dr'\rho_l^*dx}{(x^2+r'^2)^{\frac{1}{2}}}\approx8\pi^2\left(\frac{b^2}{2}-1\right)|\omega^*|I_s\lambda r^3,$$

where

$$\omega^*=\begin{cases} -|\omega^*| & \text{if } 0\le r'\le r \\ +|\omega^*| & \text{if } r\le r'\le D. \end{cases}$$

Since each domain of reverse magnetization has four near neighbors a distance D away, if θ_1 and θ_2 are small and $b\lambda\ll1$,

$$E_{np}\approx2\int_{-l}^{l}\rho_{l1}^*dx_1\int_{-l}^{l}\frac{\rho_{l2}^*dx_2}{[D^2+(x_2-x_1)^2]^{\frac{1}{2}}}=\Phi(\ln(2/\lambda))I_s^2\lambda r^3.$$

The entropy is estimated from the assumption that the total volume of the material is composed of elementary volumes V. The total number of such elementary volumes is $N_t=V_t/V$. These may be aligned either parallel or antiparallel to their prenucleation direction. The number which align themselves antiparallel at nucleation is $N_d=V_d/V$, where V_d is the volume of material which has reversed its magnetization at nucleation. The entropy change is therefore

$$\Delta S\approx-k\ln\left(\frac{N_t!}{N_d!(N_t-N_d)!}\right)\approx-N_tk\left\{p\ln\left(\frac{1}{p}\right)+(1-p)\ln\left(\frac{1}{1-p}\right)\right\},$$

where k is the Boltzmann constant and $p=V_d/V_t\approx4\pi l/3b^2l_m$. Since $N_t=3V_t/4\pi r^2l$, the dimensionless parameters of Eq. (8) are

$$\gamma_0=b^2\sigma_0/rI_s^2,$$

$$\gamma_n=f(b)b^3\omega^{*2}/I_s^2,$$

$$\gamma_p=\Psi(\ln(2/\lambda))+8\pi^2\left(\frac{b^2}{2}-1\right)(\cos\theta_1-\cos\theta_2),$$

$$\gamma_w=\frac{\pi^2}{a}\frac{\sigma_w}{I_s^2},$$

$$\gamma_H=\frac{4\pi}{3}\frac{H}{I_s}(\cos\alpha_1+\cos\alpha_2),$$

$$\gamma_S=\frac{3b^2kT}{4\pi A_slI_s^2}\left\{p\ln\left(\frac{1}{p}\right)+(1-p)\ln\left(\frac{1}{1-p}\right)\right\}.$$

It should be noted that the poles on the Bloch-wall surfaces will not be as large as was assumed in the calculation of the terms E_d, E_p, and E_{np}. This results from a deflection of the magnetic moments in the vicinity of the wall away from the easy magnetization direction. They are deflected against the anisotropy forces by the small transverse-field component associated with the Bloch-wall poles. A so-called μ^* correction[30] should, therefore, be made to these terms. Such a correction would, however, only alter the parameter γ_p. Since γ_p is eliminated through the condition of optimum periodicity area D^2, the μ^* correction will not affect the value of H_n.

APPENDIX V

The surface energy density σ_0 for a grain boundary of area $\pi(L'/2)^2$ can be approximated by calculating

$$\sigma_0=-\tfrac{1}{2}\int_0^L\mathbf{H}\cdot\mathbf{I}_sdz$$

along an axis normal to the boundary through its center. The magnetic field along this axis due to the surface poles of density ω^* is

$$H_z=-\int\frac{\omega^* dS}{z^2[1+(r'/2)^2]^{\frac{3}{2}}}=-2\pi\omega^*\left\{1-\frac{z}{(z^2+L'^2/4)^{\frac{1}{2}}}\right\},$$

where r' is the distance from the foot of the axis to the element of area dS. The surface energy density then becomes

$$\sigma_0=\pi\omega^{*2}LG;\quad G=\{1+(L'/2L)-[1+(L'/2L)^2]^{\frac{1}{2}}\}.$$

If $L'=L$, $G=\frac{1}{3}$. If only those grain boundaries which are nearly perpendicular to the applied field are considered, θ_1 and θ_2 are each less than 45°, and the μ^* correction to σ_0 will be small. It is therefore neglected in this approximation.

PHYSICAL REVIEW VOLUME 95, NUMBER 4 AUGUST 15, 1954

Magnetic and Thermal Properties of Chromic Methylamine Alum Below 1°K*

R. P. HUDSON AND C. K. MCLANE†
National Bureau of Standards, Washington, D. C.
(Received April 9, 1954)

The earlier measurements of de Klerk and Hudson on a spherical mass of small crystals of chromic methylamine alum have been repeated, and extended, using a one-inch sphere ground from a large single crystal. The variation of susceptibility with entropy follows closely—down to 0.1°K—the predictions of the theory of Hebb and Purcell when a suitable choice is made for the value of δ, the splitting between the two spin-doublets in the ground level of the Cr^{+++} ion. It is found that $\delta/k=0.269\pm0.003$ degree.

Measurements have been made of the ballistic susceptibility χ, remanent magnetic moment Σ, and the in-phase and out-of-phase components of the ac susceptibility, χ' and χ'', respectively (these latter being measured at both 150 cps and 210 cps). The variation of χ' with entropy S is found to agree closely with that reported for the powder specimen, except in the region of the susceptibility maximum where the behavior appears to depend upon the rate of precooling the specimen.

At approximately the same entropy as that corresponding to maximum χ', χ'' shows an extremely sharp maximum. The ballistic susceptibility depends upon the measuring field in the region of the maximum; remanence appears here and goes through a maximum as the entropy is reduced. The remanence maximum is found at a lower entropy the larger is the measuring field. Associated with this hysteresis are very marked "time-effects" in the adjustment of the magnetization to a change in measuring field, as encountered in tracing out hysteresis loops.

Measurements of the susceptibility in superimposed steady magnetic fields of 0–500 oersted show unusual behavior below the Curie point and suggest the existence of anisotropy. For application of the field along a cubic axis, a magnetization of about one-half the saturation value appears to have special significance; this value is attained in fields as small as 150 oersted, but increasing the field up to about 500 oersted produces little further change in the magnetization.

I. INTRODUCTION

THE magnetic and thermal properties of chromic methylamine alum, $Cr(CH_3NH_3)\cdot(SO_4)_2\cdot 12H_2O$, below 1°K were first described in an article by de Klerk and Hudson[1] (hereinafter referred to as A) dealing with adiabatic demagnetization experiments upon a powder specimen. The reasons for the interest in the properties of this particular salt are given in A. The present work concerns similar experiments made upon single-crystal specimens, wherein the magnetic properties might reasonably be supposed to be somewhat simple and more readily yielding to theoretical treatment. Independent measurements on this same salt have also been reported recently by Gardner and Kurti,[2] and by Steenland.[3]

II. APPARATUS

The salt specimen comprised a one-inch diameter sphere ground from a large single crystal.[4] This was mounted on a soft glass pedestal within a soft glass vacuum case as shown in Fig. 1. The crystal A rests on three raised points and is securely tied to the platform B by means of a nylon thread passing through holes in a polystyrene ring C and underneath B. The support D is a thin-walled glass tube with a rough ground joint at each end. Four flats were ground off the male part of each joint in order to diminish the area of thermal contact without impairing the rigidity or axial alignment of the assembly.

The vacuum case E is closed at the lower end by a plug F which constitutes another ground joint, and this is sealed by means of a glycerine-*n*-propanol mixture.[5] It is essential, of course, that this joint be tight to liquid helium II. The case E may be evacuated through

* A brief summary of this work was presented at the Third International Conference on Low Temperature Physics and Chemistry at the Rice Institute, Houston, Texas, December 17–22, 1953 (unpublished).

† On a one-year leave of absence from the University of Wisconsin. Present address: Linde Air Products Company, Tonawanda, New York.

[1] D. De Klerk and R. P. Hudson, Phys. Rev. **91**, 278 (1953), hereinafter referred to as A.

[2] W. E. Gardner and N. Kurti (private communication).

[3] M. J. Steenland, in Rice Institute, Third International Conference on Low Temperature Physics and Chemistry; Abstracts of Papers, Houston, Rice Institute, 1953.

[4] We are greatly indebted to Mr. Walter Kuper for the preparation of the crystals used in this work.

[5] R. P. Hudson and C. K. McLane, Rev. Sci. Instr. **25**, 190 (1954).

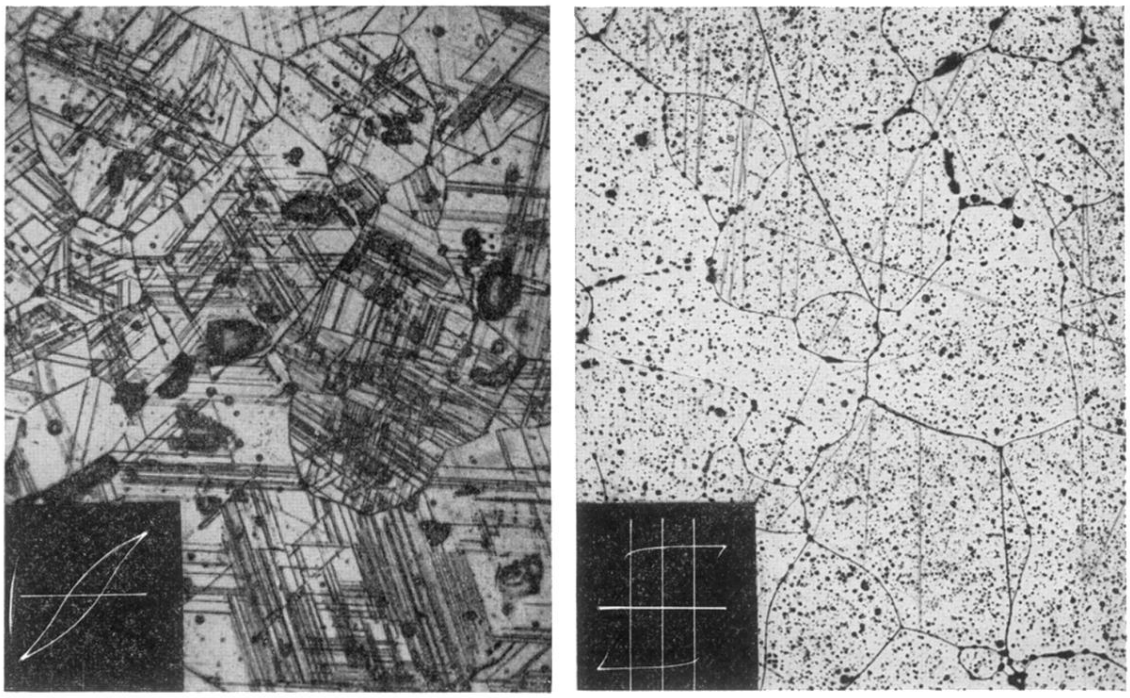

(a) (b)

FIG. 14. Microstructure and maximum-squareness-ratio B-H loop for a General Ceramics Company MF-1371-B ferrite body (a) before anneal (white light×498, $B_m = 150$ gauss, $H_m = 2.25$ oersteds) and (b) after anneal (white light×100, $B_m = 1128$ gauss, $H_m = 0.46$ oersted).